International Journal of Science and Research (IJSR)
ISSN (Online): 2319-7064
Index Copernicus Value (2013): 6.14 | Impact Factor (2013): 4.438

Dynamics of Daily Rainfall and Temperature in Makurdi

I.M. Echi[1*], E.V. Tikyaa[2], B.C. Isikwue[3]

[1]Department of Physics, University of Agriculture Makurdi, Benue State, Nigeria
[*]On sabbatical leave at: Department of Natural and Applied Sciences, Namibia University of Science and Technology, Windhoek, Namibia.

[2]Department of Physics, Federal University Dutsin-ma, Katsina State, Nigeria

[3]Department of Physics, University of Agriculture Makurdi, Benue State, Nigeria

Abstract: ***Having a detailed knowledge of rainfall and temperature dynamics is important for an adequate management of our meteorological and hydrological resources. Chaos theory being the basis for studying nonlinear dynamic systems has opened a lot of doors towards understanding complex systems in nature such as the weather. In this study the dynamics of daily rainfall and temperature in Makurdi from January 1st 1977 – December 31st 2010 is investigated using chaos theory. A variety of nonlinear techniques such as power spectrum, phase space reconstruction, Lyapunov exponents and correlation dimension are applied. The optimal delay times were calculated for rainfall and temperature using the average mutual information technique while optimal embedding dimensions were also obtained using the method of false nearest neighbors. Phase space reconstruction was carried out with these optimal values using the method of delays. The phase portraits showed geometry of distinct shapes interwoven to form spongy like structures indicating the presence of randomness and chaos in the data with that of rainfall concentrated at the origin due to the numerous zeros in the rainfall values. The correlation dimensions were estimated using the Grassberger-Procaccia algorithm and found to be 1.02 and 5.82 for the rainfall and temperature respectively while the Lyapunov exponents were calculated using Rosenstein's approach and obtained as 0.00832/day and 0.00574/day for daily rainfall and temperature respectively. The small values (υ<20) of the correlation dimensions obtained suggest the presence of chaotic behavior of low dimensions; inferring that the rainfall dynamics is dominantly governed by a minimum (maximum) of 2(18) variables while the temperature dynamics is governed by a minimum (maximum) of 6(17) variables. The positive values of the largest Lyapunov exponents confirm the presence of chaotic dynamics in rainfall and temperature records over Makurdi and suggest predictability of within 112 days and 174 days for rainfall and temperature respectively.***

Keywords: Chaos, power spectrum, phase space reconstruction, phase portrait, correlation dimension, Lyapunov exponent.

1. Introduction

Recent developments in information technology and computing ability in the last few years have made it possible for in-depth exploration of complex systems in the natural sciences. A focal issue in the exposition of complex systems is the unraveling of the structure of "disorder", a common and usually prevailing, yet neglected characteristic of many dynamical systems. The study of nonlinear systems is aimed at a new understanding of the "laws of disorder" also referred to as "the Chaos theory" or "Nonlinear dynamics". Chaos is a subset of the more general nonlinear dynamical entity [1]. For a dynamical system to be classified as chaotic, it must be generally characterized by a sensitivity to initial conditions, topologically mixing (i.e. the system must be transitive); and its periodic orbits must be dense [2]. The identification of chaos in atmospheric systems is due to an accidental discovery by Edward Lorenz, a meteorologist in 1961 when he constructed a very crude model of the convection of the atmosphere as it is heated from below by the ground. Lorenz discovered, to his greatest surprise, that his modeled atmosphere exhibited chaotic motion—which, at that time, was virtually unknown to Physics [3]. In particular, Lorenz realized that the chaotic dynamics of the atmosphere spells doom for long-term weather forecasting i.e. the best one can hope to achieve is to predict the weather a few days in advance [4]. Weather is chaotic because air is light, it has low friction and viscosity, it expands strongly when in contact with hot surfaces and it conducts heat poorly; wind induces forced convections and is never in equilibrium [5].

In modern meteorological and hydrological studies, huge emphasis is laid on time series modeling and this is used in designing, planning and forecasting of meteorological and water resource systems. Time series represents a quantitative measure of a physical process 'x(t)' recorded at time 't' which can be discrete or continuous [6]. In this paper, the dynamics of rainfall and temperature in Makurdi, Benue State, Nigeria over the last three decades is investigated. The tools of nonlinear dynamics were applied to rainfall and temperature time series and the results obtained will provide information about the dynamics of our weather so as to enable a more accurate modeling and forecasting of the weather across the country in future.

2. Theoretical Framework

The tools of nonlinear analysis employed in this work include qualitative tools such as observation of the state variables i.e. the time series plot, Power spectrum, Phase portrait and the quantitative tools which tells us the degree of chaoticity in the system such as correlation dimension and Lyapunov exponents.

2.1 Time Series Plot

Time series plot (trajectory plot) is a visual method which involves plotting the state variables of the system and

observing the trend. If they exhibit irregular, aperiodic or unpredictable behavior, then it is called chaotic. On the other hand if they exhibit a regular repeating pattern, then the system exhibits either a periodic and quasi periodic behavior [7].

2.2 Power Spectrum

The power spectrum of a signal shows how a signal's power is distributed throughout the frequency domain. The power spectrum is the square of the absolute value of the Fast Fourier Transform of the time series. Chaotic signals are characterized by the presence of wide broadband noise in their power spectrum, or in other words its power spectrum is expressed in terms of oscillations with a continuum of frequencies [8].

2.3 Phase Portrait

A phase portrait is a two-dimensional projection of the phase-space. It represents each of the state variable's instantaneous state to each other. Chaotic and other motions can be distinguished visually from each other according to the description in Table 1 [7].

Table 1: Solutions of dynamic systems

Solution	**Fixed**	**Periodic**	**Quasi Periodic**	**Chaotic**
Nature of Phase portrait	Point	Closed curve	Torus	Distinct Shapes

2.4 Correlation Dimension

The correlation dimension actually gives a measure of complexity for the underlying attractor of the system by measuring the number of "degrees of freedom" excited by the system [9]. For any set of M points in an *m*-dimensional phase space, the correlation integral or correlation sum (spatial correlation of points) *C*(r) is computed by the equation [10]:

$$C_m(r) = \lim_{N\to\infty} \frac{2}{N(N-1)} \sum_{i=1}^{M} \sum_{j=i+1}^{M} H\left(r - \|\vec{x_i} - \vec{x_j}\|\right) \quad (1)$$

Where H(*x*) is the Heaviside function and $\|\ldots\|$ is the Euclidean norm while r is the tolerance distance (scaling parameter). The value of r should be smaller than the diameter of the set (which is considered to be equal to one) and larger than the mean nearest neighbor distance [11]. The correlation integral measures the fraction of the total number of pairs of phase points that are within a distance r from each other. Stochastic time series obey the power law [12]:

$$C(r) \sim r^m \quad (2)$$

While for chaotic time series, the correlation integral power law for small values of r takes the form:

$$C(r) \sim r^{\nu} \quad (3)$$

Hence, the correlation dimension ν is given by:

$$\nu = \lim_{r\to 0} \lim_{M\to\infty} \frac{\log C(r)}{\log r} \quad (4)$$

This implies that for a sufficiently large number of points that are evenly distribution, a log-log graph of the correlation integral versus the scaling parameter, r will yield an estimate of the correlation dimension *ν,* which is computed from a least-square fit of a straight line over a length scale of r [10]. Chaotic systems usually have low and fractal values of correlation dimension i.e. ν <20 and its correlation exponent curve for a range of values of embedding dimension (say m = 2 to 20) usually saturates at values beyond its actual embedding dimension [12]. The nearest integer above the saturation value is generally considered to provide the minimum number of phase-space or variables necessary to model the dynamics of the attractor. The value of the embedding dimension at which the saturation of the correlation exponent occurs generally provides an upper bound on the number of variables sufficient to model the dynamics [13]. However, if the correlation exponent increases without bound with increase in the embedding dimension, then the system under investigation is generally considered as stochastic [14].

2.5 Lyapunov Exponents

Lyapunov exponents (λ) are the average rates of exponential divergence or convergence of nearby orbits in phase space. It shows the long term behavior of the time series and is a fundamental property that characterizes the rate of separation of infinitesimally close trajectories [15]. The method used in computing the largest Lyapunov exponent was developed by Rosenstein *et al* [16] and it computes the largest Lyapunov exponent for small data sets more accurately. This method proceeds by assuming the jth pair of nearest neighbors diverges approximately at a rate given by the largest Lyapunov exponent:

$$d_j(i) \approx C_j(i) e^{\lambda(idt)} \quad (5)$$

where C_j is the initial separation (i.e. $d_j(0)$) and dt is the sampling interval. By taking the natural logarithm of both sides, they obtained the equation:

$$\ln d_j(i) \approx \ln C_j(i) + \lambda(idt) \quad (6)$$

If a typical plot (solid curve) of the average exponential divergence $\ln d_j(i)$ against $i.dt$ is made; the slope of the dashed line fitted to the curves has a slope equal to the theoretical value of λ (the largest Lyapunov exponent). This can easily be calculated by using a regression line with the method of least squares. Lyapunov exponents quantify the sensitivity to initial conditions and its sign is interpreted as shown in Table **2**[12]:

Table 2: Possible types of dynamical systems and the corresponding largest Lyapunov exponents

Largest Lyapunov exponent (λ_1)	$\lambda_1 < 0$	$\lambda_1 = 0$	$0 < \lambda_1 < \infty$	$\lambda_1 = \infty$
Dynamics of the system	Stable fixed point (periodic)	Stable limit cycle (quasi-periodic)	Deterministic chaos	Noise (Random motion)

The Lyapunov (e-folding) time or predictability T is the time within which it is possible to predict the system forward and can be computed in terms of the largest Lyapunov exponent λ_1 using the expression [17]:

$$T = \frac{dt}{\lambda} \quad (7)$$

where dt is the sampling interval.

2.6 Phase Space Reconstruction

In order to carry out nonlinear analysis of the data, phase space reconstruction has to be carried out on the data so as to draw out a multidimensional description of state space dynamics from the time series data of a single dynamical variable, and generalize the qualitative measures of chaotic behavior. Another physical reason for a possible phase space reconstruction is that nonlinear systems are usually characterized by self-interaction, so that a single variable may carry information about the whole system [16]. The method of delay (MOD) is used in this research work [15],[18].

For a time series $\{x_1, x_2,\ldots,x_N\}$, where N is the number of observations, the attractor can be reconstructed in a m-dimensional phase space of delay coordinates by forming the vectors:

$$X_n = [x_n, x_{n+\tau}, x_{n+2\tau}, \cdots, x_{n+(m-1)\tau}] \quad (8)$$

where τ is the delay time, and the integer m (the embedding dimension) must be chosen appropriately. In practical terms, the delay time (or time lag) τ must be the shortest time over which there are clearly measurable variations in the observable.

$$\tau = idt \quad (9)$$

where dt is the sampling interval and i is the lag length.

In this study, the delay time τ is evaluated using the method of Average Mutual Information (AMI) postulated by Cellucci *et al.* The average mutual information is defined by [19]:

$$I(\tau) = -\sum_{ij}^{N} P_{ij}(\tau)\, ln \frac{P_{ij}(\tau)}{P_i(\tau)P_j(\tau)} \quad (10)$$

where $P_i(\tau)$ and $P_j(\tau)$ are the probabilities of finding x_i in the ith and $x_{i+\tau}$in the jth interval, and $P_{ij}(\tau)$ is their joint probability. A plot of $I(\tau)$ versus the lag length τ is made and the first local minimum of the curve corresponds to the optimum selection of the delay time τ.

The minimum embedding dimension, m for phase space reconstruction in this work is computed using the method of "**F**alse **N**earest **N**eighbors (FNN)" developed by Kennel *et al.* [20]. This method works by checking the neighborhood of points embedded in projection manifolds of increasing dimension and eliminating 'false neighbors.' This means that points apparently lying close together due to the projection are separated by choosing higher embedding dimensions. A natural criterion for catching embedding errors is that the increase in distance between two neighbored points is large when going from dimension m to m+1. This criterion is achieved by designating as a false nearest neighbor any neighbor for which the following is valid:

$$\left[\frac{R_{m+1}^2(n,r) - R_m^2(n,r)}{R_m^2(n,r)}\right]^{\frac{1}{2}} = \frac{|x(n+m\tau) - x^{(r)}(n+m\tau)|}{R_m^2(n,r)} > R_{tol} \quad (11)$$

where R_m^2 is defined as:

$$R_m^2(n,r) = \sum_{k=0}^{m-1}\left[x(n+k\tau) - x^{(r)}(n+k\tau)\right]^2 \quad (12)$$

and

$$R_{m+1}^2(n,r) = R_m^2(n,r) + \left[x(n+k\tau) - x^{(r)}(n+k\tau)\right]^2 \quad (13)$$

$x^{(r)}(n)$ is the rth nearest neighbor of x(n). R_m denotes the Euclidean distance (norm) in phase space between nearest neighbors with embedding dimension m, and R_{tol} is the tolerance threshold. The R_{tol} criterion by itself is not sufficient for determining a proper embedding dimension as a problem turns out if a point is a nearest neighbor of another without necessarily being close to it thus causing the number of false nearest neighbors to increase at higher dimensions. In order to tackle this problem, a further criterion is introduced; the loneliness criterion. It is represented by the loneliness tolerance threshold, A_{tol}.
The condition for the loneliness criterion is:

$$\frac{R_{m+1}(n)}{\sigma^2} > A_{tol} \quad (15)$$

where σ is the variance of the data set.

$$\sigma^2 = \frac{1}{N}\sum_{n=1}^{N}[x(n) - \bar{x}]^2, \bar{x} = \frac{1}{N}\sum_{n=1}^{N} x(n) \quad (16)$$

The output produced by the function in this method is a plot of the percentage of FNN versus increasing embedding dimension and has a monotonic decreasing curve. The minimum embedding dimension usually can be found where the percentage of FNN drops to almost zero or a minimum value [20]. In topological terms, each vector in phase space can be considered to provide the coordinates of a point in an m-dimensional phase space, and these vectors also provide a way to reproduce the dynamics of the real unknown system [1].

3. The Study Area and Data Used

Makurdi is the capital of Benue state in the North-central region of Nigeria. The city has coordinates $7°43'50''N, 8°32'10''E$ and is located on the Banks of River Benue a major tributary of the Niger River. Its landscape is largely dominated by the Guinea savannah vegetation and experiences two dominant seasons: the rainy and dry season [21].

Figure 1: Map of Benue state showing the location of the study area (Makurdi). Source: Google maps [22].

The data used in this research was obtained from the International Institute for Tropical Agriculture (IITA) Ibadan, Nigeria. It comprises of secondary data made up of daily averages of rainfall (mm) and average temperature (°C) recorded over Makurdi from 1st January, 1977 to 31st December 2010, a period of thirty four years.

4. Results and Discussion

The statistics of rainfall (mm) and temperature (℃) are displayed in Tables 3 and 4 below:

Table 3: Statistics of daily rainfall time series in Makurdi

Statistic	Value
No. of data	12,418
No. of zeros	9,670
Mean(mm)	3.24
Standard Deviation(mm)	10.14
Variance(mm)	102.87
Coefficient of Variation	3.13
Maximum value(mm)	149.30
Minimum value(mm)	0.00
Kurtosis	34.24
Skewness	4.84

Table 4: Statistics of daily Average temperature time series in Makurdi

Statistic	Value
No. of data	12,418
No. of zeros	0
Mean(℃)	28.59
Standard Deviation(℃)	1.99
Variance(℃)	3.97
Coefficient of Variation	0.07
Maximum value(℃)	34.50
Minimum value(℃)	21.70
Kurtosis	3.01
Skewness	0.15

Figure 2 shows the time series plot of rainfall (mm) and temperature (℃) in Makurdi over three decades.

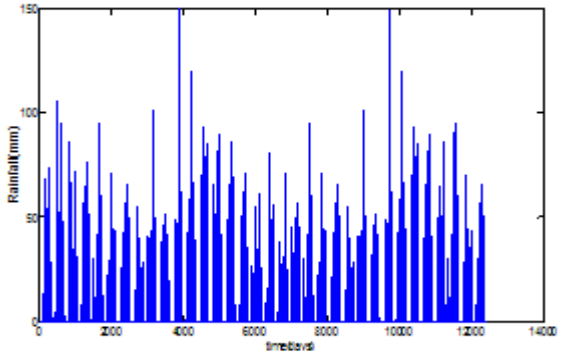

(a)

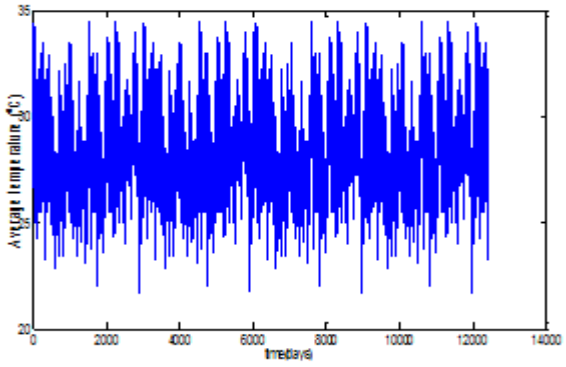

(b)

Figure 2: Time series for: (a) Rainfall and (b) Temperature in Makurdi.

Figure 3 shows the power spectra of rainfall and temperature time series observed in Makurdi. Both spectra show fractal (random) behavior with broadband noise and no dominant peaks. The daily rainfall time series has a mean orbital period of 182.62 days while the daily temperature time series has a mean orbital period of 126.71 days. The mean orbital period is the reciprocal of the mean (peak) frequency of the power spectrum [16].

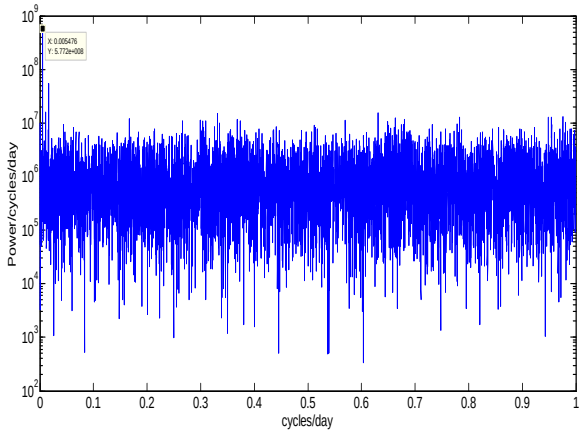

(a)

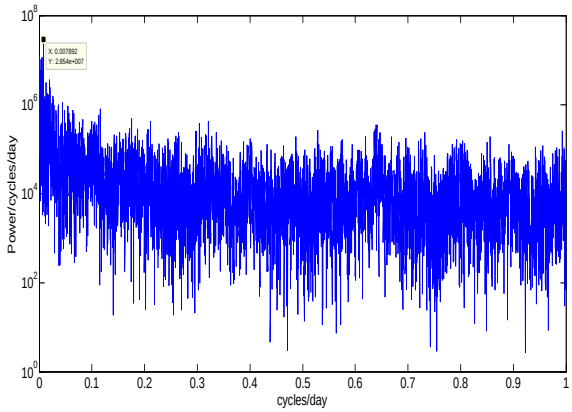

(b)

Figure 3: Power spectrum for: (a) Rainfall and (b) Temperature in Makurdi.

Figure 4 shows the estimation of delay time using the method of average mutual information (AMI). A delay time of 2days was calculated for rainfall data while a delay time of 5days was estimated for the temperature dataset.

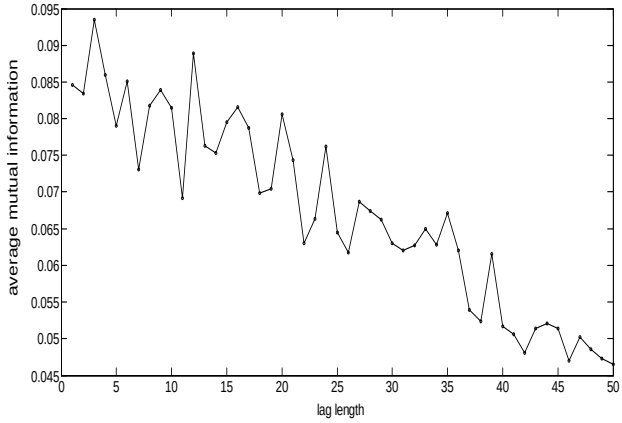

(a)

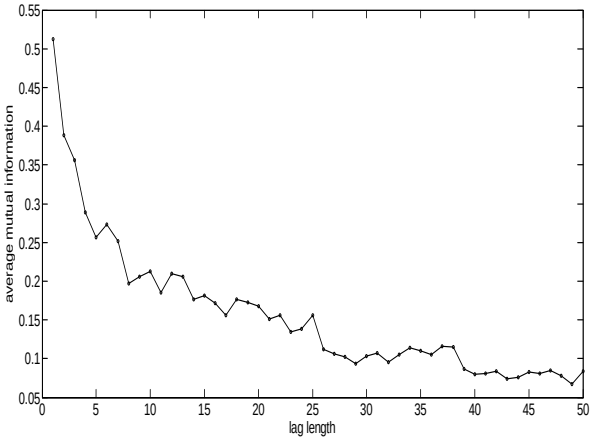

(b)

Figure 4: AMI function for: (a) Rainfall (τ=2days) and (b) Temperature (τ =5days)

Figure 5 illustrates the determination of the optimal embedding dimension using the method of false nearest neighbors (FNN). The rainfall data was found to have an embedding dimension of nine (m=9) while the temperature dataset has an optimal embedding dimension of five (m=5).

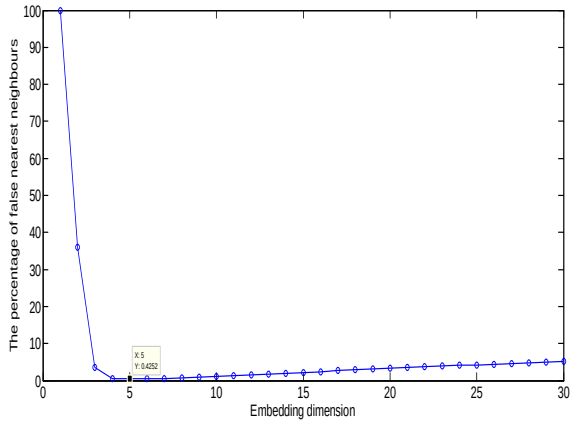

(a)

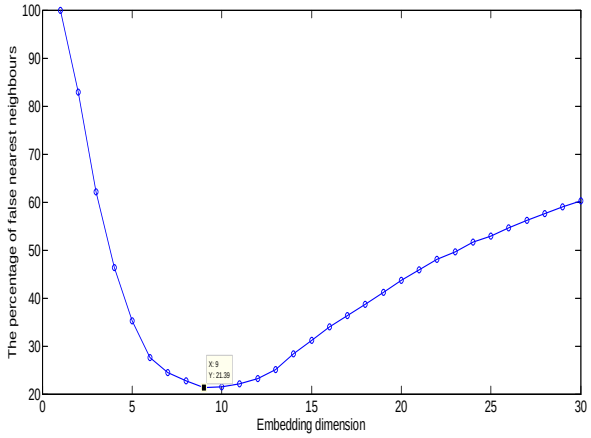

(b)

Figure 5: Percentage of FNN for: (a) Rainfall (m=9) and (b) Temperature (m=5)

Figure 6 shows the phase portraits of the reconstructed phase spaces for rainfall and temperature using the delay time and embedding dimensions calculated. Both show spongy like geometry of distinct shapes implying the presence of random and chaotic dynamics in the rainfall and temperature time series with that of rainfall concentrated at the origin due to the numerous zeros in the rainfall values.

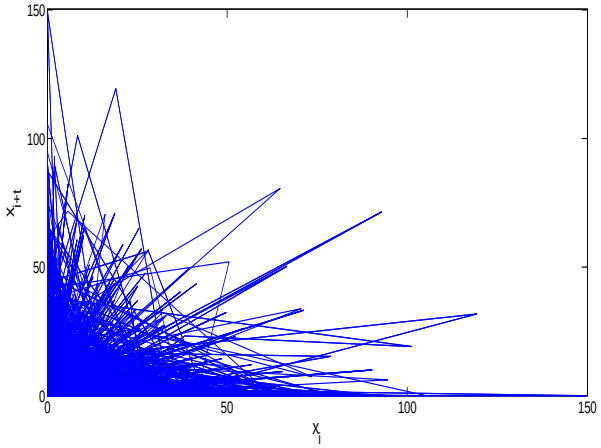

(a)

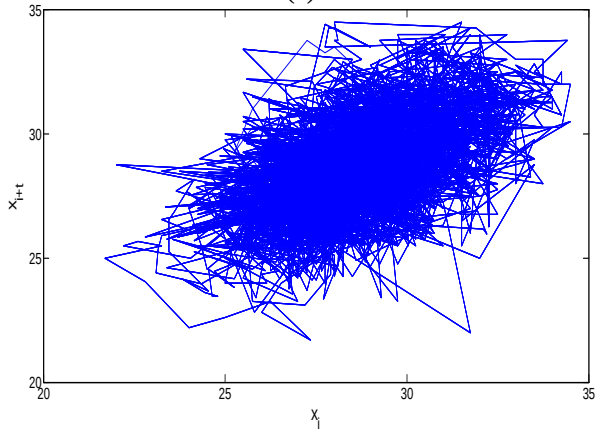

(b)

Figure 6: Phase portrait for: (a) Rainfall and (b) Temperature in Makurdi

The correlation functions were calculated for the rainfall and temperature datasets using the delay times τ =2 and τ =5 respectively for increasing embedding dimensions, *m*, from 1 to 20.

Figure 7 shows the relationship between the correlation function *C(r)* and the radius *r* (i.e. $\log C(r)$ versus $\log r$) for increasing embedding dimension *m*. The relationship between the correlation exponents and the embedding dimension values *m* is shown in figure 8. The correlation exponents were obtained from the $\log C(r)$ vs $\log r$ plot and are the slopes estimated from the most linear portion of the correlation integral graph plotted on a logarithmic scale [23].

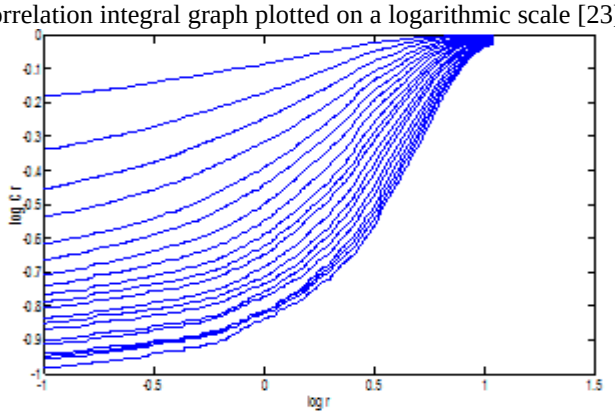

(a)

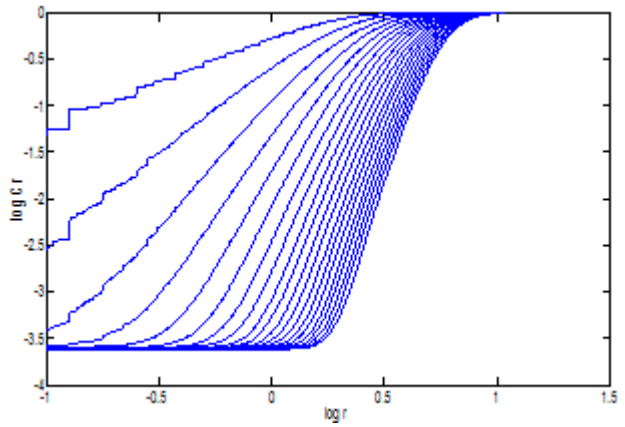

(b)

Figure 7: $\log C(r)$ versus $\log r$ plots for: (a) Rainfall (b) Temperature data in Makurdi.

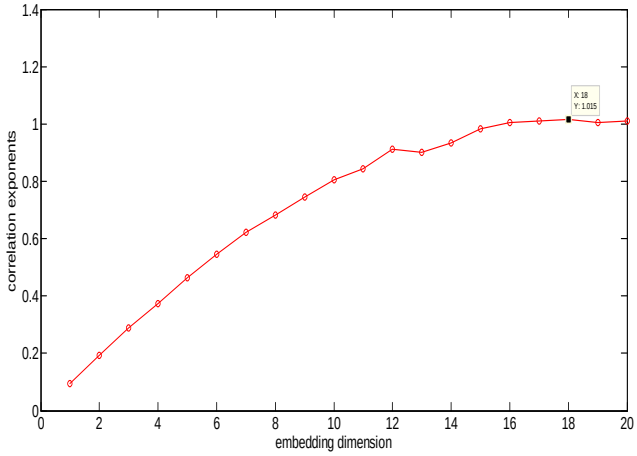

(a)

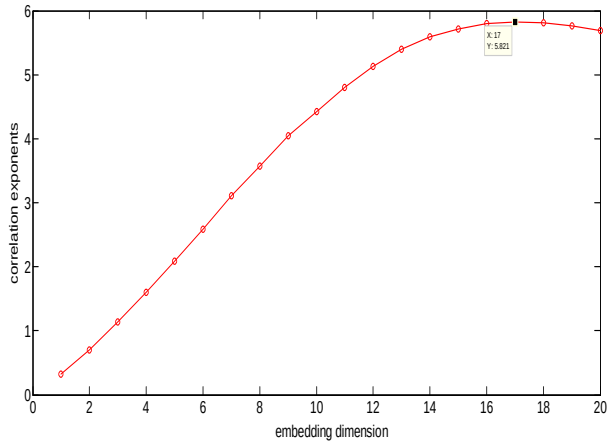

(b)

Figure 8: Relation between correlation exponent and embedding dimension *m* for: (a) Rainfall (υ =1.02) and (b) Temperature (υ =5.82)

From the figures above, it is observed that the value of the correlation exponents increase with the embedding dimension up to certain value and then saturates beyond it. The saturation of the correlation exponent beyond a certain embedding dimension value is the indication of an existence of chaotic dynamics. The saturated correlation dimension is 1.02 for rainfall and 5.82 for average temperature. These low (<20) values of correlation dimension suggest that there is a possible presence of chaotic behavior and fractal characteristics in the rainfall and temperature time series. The underestimation of correlation dimensions in the rainfall time series may be due to higher number of zero values (i.e. 9760; Table 3) in the rainfall data [24]. Similarly from the correlation exponent curves in figure 8, we can infer that the daily rainfall in Makurdi requires a minimum (maximum) of 2(18) independent variables to model its dynamics while a minimum (maximum) of 6(17) independent variables are needed to model the dynamics of daily average temperature in Makurdi.

Rosenstein's algorithm was applied for the estimation of the largest Lyapunov exponent using the delay time and embedding dimension earlier obtained. Figures 9 shows the curve for the exponential divergence (stretching factor) *d(k)* versus the number of iterations *k=i.dt* (Lyapunov spectrum). The slope value of the rising part of the curve corresponds to the largest Lyapunov exponent. This is obtained from the least-squares line fit. Rainfall time series was found to have a largest Lyapunov exponent of 0.0632 while the temperature time series has a largest Lyapunov exponent of 0.00572. The positive values of the Lyapunov exponents indicate a strong signature of chaos in rainfall and temperature in Makurdi over the last 34 years.

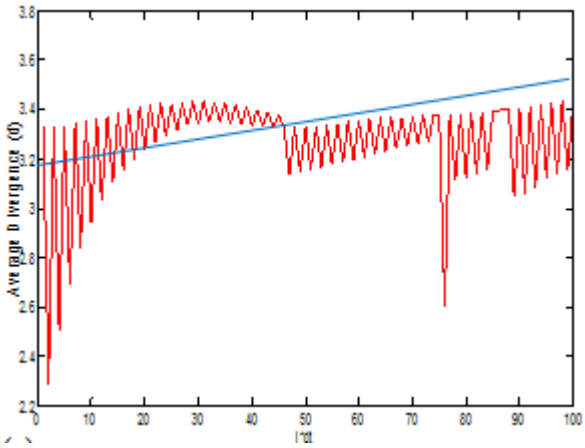

(a)

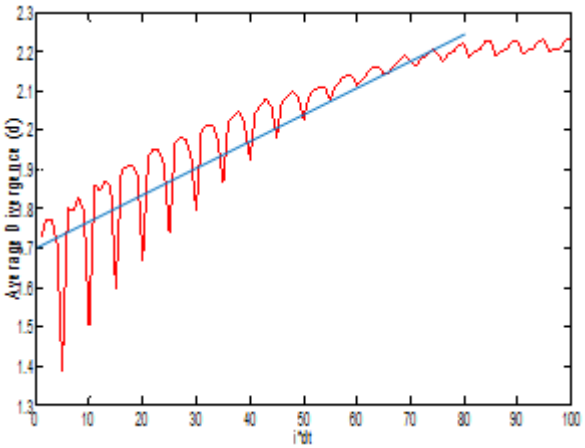

(b)

Figure 9: Estimation of the largest Lyapunov exponent from the Lyapunov spectrum for: (a) rainfall (λ = 0.00832) and (b) Temperature (λ = 0.00574)

The inverse of the largest Lyapunov exponent estimates predictability (error doubling time) of time series, hence we

can say that the daily rainfall in Makurdi is accurately predictable as from 1st January 2011 for the next 112 days while the daily average temperature was found to be predictable for the next 174 days.

5. Conclusion

In this work, the dynamics of daily rainfall and temperature in Makurdi over the last three decades was investigated using the tools of nonlinear dynamics. The outcome of this analysis confirmed that both rainfall and temperature in Makurdi exhibit chaotic behavior and while the daily rainfall time series requires a minimum of two (2) and maximum of eighteen (18) variables for the modeling of its dynamics, the daily temperature time series requires a minimum of six (6) and maximum of seventeen (17) variables for the modeling of its dynamics. It was also estimated via the largest Lyapunov exponents that the daily rainfall and temperature over Makurdi are predictable for the next 112 and 174 days respectively.

6. Acknowledgements

One of the authors wishes to acknowledge the authorities of the Federal University Dutsin-ma, Katsina State, Nigeria for supporting him technically and financially during the period of this research.

References

[1] A. Karytinos, "A Chaos Theory and Nonlinear Dynamics Approach to the Analysis of Financial Series: A Comparative Study of Athens and London Stock Markets," A dissertation presented for the Doctor of Philosophy Degree Warwick Business School, University of Warwick, UK, pp.4-21, 1999.
[2] B. Hasselblatt, and K. Anatole, A First Course in Dynamics: With a Panorama of Recent Developments, Cambridge University Press, Cambridge, 2003.
[3] E. Lorenz, "Dimension of weather and climate attractors." Letters to Nature, 353, pp.241-244, 1961.
[4] E. Lorenz, "Deterministic non-periodic flow," Journal of the Atmospheric Sciences, 20(2), p.41, 1963.
[5] X. Zeng, "Chaos Theory and its Application in the Atmosphere," Atmospheric Science, 504, pp.5-44, 1992.
[6] T. Fathima and V. Jothiprakash, "Behavioural Analysis of a Time Series-A Chaotic Approach," Sâadhanâ, 39(3), pp. 659-676, 2014.
[7] B. Ozer and E. Akin, "Tools for Detecting Chaos," Sau Fen Bilimleri EnstitusuDergisi, 9(1), pp.60-66, 2005.
[8] H. Shannon, "Power Spectrum in MATLAB," *BitWeenie: digital signal processing, par. 3, Feb. 21, 2013.* Available: http://www.Bit Weenie.html. [Accessed: August 4, 2013].
[9] D. Rothman, "Nonlinear dynamics I: chaos-Lyapunov exponents," MIT open courseware on Dynamics and Relativity, par.4, Jan. 7, 2012. Available: http://archive.org/details /flooved1828. [Accessed: May 21, 2012].
[10] P. Grassberger and I. Procaccia, "Characterisation of Strange Attractors," Phys. Rev. lett., 50, pp.346-349, 1983.
[11] L. Smith, "Intrinsic limits on dimension calculations," Physics Letters A,133, pp.283-288, 1988.
[12] J. Rasoul, G. Mohammad, and S. Abolfaz, "Dynamics of Rainfall in Ramsar," Journal of Applied Science and Agriculture, 9(4), pp.1371-1378, 2014.
[13] K. Fraedrich, "Estimating the dimensions of weather and climate attractors," J. Armos. Set. 43(5), pp.419-432, 1986.
[14] B. Sivakumar, "Rainfall dynamics at different temporal scales: A chaotic perspective," Hydrol. and Earth Sys. Sci., 5(4), pp.645–651, 2001.
[15] F. Takens, "Detecting Strange Attractors in Turbulence." Lecture Notes in Mathematics, 898, p.366, 1981.
[16] M. Rosenstein, J. Collins, and C. De Luca, "A practical method for calculating largest Lyapunov exponents from small data sets," Physica D, 65, pp.117-134, 1992.
[17] J. Stehlík, **"**Searching for Chaos in Rainfall and Temperature Records – a Nonlinear Analysis of Time Series from an Experimental Basin**,"** Na Sabatce, 17(143), p.4, 2006.
[18] N. Packard, J. Crutchfield, J. Farmer, and R. Shaw, "Geometry from a Time Series," Phys. Rev. Lett., 45, p.712, 1980.
[19] C. Cellucci, A. Albano, P. Rapp, "Comparative study of embedding methods," Phys. Review E, 67(6), pp.1 -13, 2003.
[20] M. Kennel, R. Brown and H. Abarbanel, "Determining embedding dimension for phase-space reconstruction using a geometrical construction," Phys. Rev. A, 45(6), pp.3403-3411, 1992.
[21] http://en.wikipedia.org/wiki/Makurdi, [Accessed: June 17, 2015].
[22] https://www.google.com.ng/maps/ place/Makurdi/@7.7290891,8.555926, 13z/data.[Accessed: June 17, 2015].
[23] B. Shivamoggi, Nonlinear dynamics and chaotic phenomena: An introduction, Kluwer Academic Publishers, Netherlands, 1997.
[24] B. Sivakumar, R. Berndtsson, J. Olsson and K. Jinno, "Evidence of chaos in the rainfall-runoff process," Journal of Hydrological Sciences, 46(1), pp. 131-145, 2001.